Article

Gas-Phase Synthesis of the Homo and Hetero Organocuprate Anions [MeCuMe], [EtCuEt], and [MeCuR]

Nicole Rijs, George N. Khairallah, Tom Waters, and Richard A. J. O'Hair

J. Am. Chem. Soc., **2008**, 130 (3), 1069-1079 • DOI: 10.1021/ja0773397

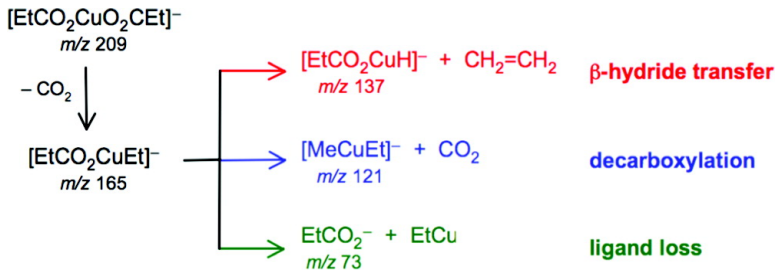

More About This Article

Additional resources and features associated with this article are available within the HTML version:

- Supporting Information
- Links to the 4 articles that cite this article, as of the time of this article download
- Access to high resolution figures
- Links to articles and content related to this article
- Copyright permission to reproduce figures and/or text from this article

View the Full Text HTML

J|A|C|S
ARTICLES
Published on Web 01/01/2008

Gas-Phase Synthesis of the Homo and Hetero Organocuprate Anions $[MeCuMe]^-$, $[EtCuEt]^-$, and $[MeCuR]^-$

Nicole Rijs,[†,‡] George N. Khairallah,[†,‡,§] Tom Waters,[†,‡] and Richard A. J. O'Hair*[,†,‡,§]

School of Chemistry, Bio21 Institute of Molecular Science and Biotechnology, and ARC Centre of Excellence in Free Radical Chemistry and Biotechnology, University of Melbourne, Victoria 3010, Australia

Received September 21, 2007; E-mail: rohair@unimelb.edu.au

Abstract: The homocuprates $[MeCuMe]^-$ and $[EtCuEt]^-$ were generated in the gas phase by double decarboxylation of the copper carboxylate centers $[MeCO_2CuO_2CMe]^-$ and $[EtCO_2CuO_2CEt]^-$, respectively. The same strategy was explored for generating the heterocuprates $[MeCuR]^-$ from $[MeCO_2CuO_2CR]^-$ (R = Et, Pr, *i*Pr, *t*Bu, allyl, benzyl, Ph). The formation of these organocuprates was examined by multistage mass spectrometry experiments, including collision-induced dissociation and ion−molecule reactions, and theoretically by density functional theory. A number of side reactions were observed to be in competition with the second stage of decarboxylation, including loss of the anionic carboxylate ligand and loss of neutral alkene via β-hydride transfer elimination. Interpretation of decarboxylation of the heterocarboxylates $[MeCO_2CuO_2CR]^-$ was more complex because of the possibility of decarboxylation occurring at either of the two different carboxylate ligands and giving rise to the possible isomers $[MeCuO_2CR]^-$ or $[MeCO_2CuR]^-$. Ion−molecule reactions of the products of initial decarboxylation with allyl iodide resulted in C−C coupling to produce the ionic products $[ICuO_2CR]^-$ or $[MeCO_2CuI]^-$, which provided insights into the relative population of the isomers, and indicated that the site of decarboxylation was dependent on R. For example, $[MeCO_2CuO_2CtBu]^-$ underwent decarboxylation at $MeCO_2^-$ to give $[MeCuO_2CtBu]^-$, while $[MeCO_2CuO_2CCH_2Ph]^-$ underwent decarboxylation at $PhCH_2CO_2^-$ to give $[MeCO_2CuCH_2Ph]^-$. Each of the heterocuprates $[MeCuR]^-$ (R = Et, Pr, *i*Pr, allyl, benzyl, Ph) could be generated by the double decarboxylation strategy. However, when R = *t*Bu, intermediate $[MeCuO_2CtBu]^-$ only underwent loss of $tBuCO_2^-$, a consequence of the steric bulk of *t*Bu disfavoring decarboxylation and stabilizing the competing channel of carboxylate anion loss. Detailed DFT calculations were carried out on the potential energy surfaces for the first and second decarboxylation reactions of all homo- and heterocuprates, as well as possible competing reactions. These reveal that in all cases the first decarboxylation reaction is favored over loss of the carboxylate ligand. In contrast, other reactions such as carboxylate ligand loss and β-hydride transfer become more competitive with the second decarboxylation reaction.

Introduction

Organocopper reagents are among the most widely used organometallic reagents in organic synthesis.[1] Organocuprates, formulated as "R_2CuLi" and known as Gilman reagents, have proven useful in a range of C−C bond coupling reactions.[2] However, despite more than 50 years of use and a number of key recent theoretical studies,[3] there is still a lack of detailed mechanistic insights into their reactivity and specific mode of action.[4,5] Furthermore, their use is hampered by decomposition reactions, which can compete with the desired coupling reaction, thereby limiting the temperature range at which coupling reactions can be carried out. The decomposition reactions can be complex and can give rise to several products, including copper nanoparticles, which can in turn catalyze further decomposition.[6−9] In fact, Bertz et al. noted that even subtle factors such as the nature of the surface of the reaction vessel are important and suggest that "scrupulous attention to experi-

[†] School of Chemistry.
[‡] Bio21 Institute of Molecular Science and Biotechnology.
[§] ARC Centre of Excellence in Free Radical Chemistry and Biotechnology.

(1) For reviews and monographs on organocopper species, see: (a) *Modern Organocopper Chemistry*; Krause, N., Ed.; Wiley-VCH: Weinheim, Germany, 2002. (b) Lipshutz, B. H. In *Organometallics in Synthesis;* Schlosser, M., Ed.; Wiley: Chichester, U.K., 1994; pp 283−382. (c) *Organocopper Reagents: A Practical Approach;* Taylor, R. J. K., Ed.; Oxford University Press: Oxford, U.K., 1994.

(2) For an excellent account of Gilman's research, see: Eisch, J. J. *Organometallics* **2002**, *21*, 5439.

(3) Nakamura has carried out extensive theoretical studies. For a selection of key recent articles, see: (a) Yamanaka, M.; Kato, S.; Nakamura, E. *J. Am. Chem. Soc.* **2004**, *126*, 6287. (b) Nakanishi, W.; Yamanaka, M.; Nakamura, E. *J. Am. Chem. Soc.* **2005**, *127*, 1446. (c) Yamanaka, M.; Nakamura, E. *J. Am. Chem. Soc.* **2005**, *127*, 4697. (d) Yoshikai, N.; Yamashita, T.; Nakamura, E. *Angew. Chem., Int. Ed.* **2005**, *44*, 4721. (e) Norinder, J.; Backvall, J.-E.; Yoshikai, N.; Nakamura, E. *Organometallics* **2006**, *25*, 2129.

(4) For an excellent review focusing on mechanistic aspects, see: Nakamura, E.; Mori, S. *Angew. Chem., Int. Ed.* **2000**, *39*, 3751.

(5) Recent experimental and theoretical studies provide evidence for the formation of Cu(III) intermediates in C−C bond coupling reactions. (a) Bertz, S. H.; Cope, S.; Murphy, M.; Ogle, C. A.; Taylor, B. J. *J. Am. Chem. Soc.* **2007**, *129*, 7208. (b) Hu, H.; Snyder, J. P. *J. Am. Chem. Soc.* **2007**, *129*, 7210.

10.1021/ja0773397 CCC: $40.75

Scheme 1

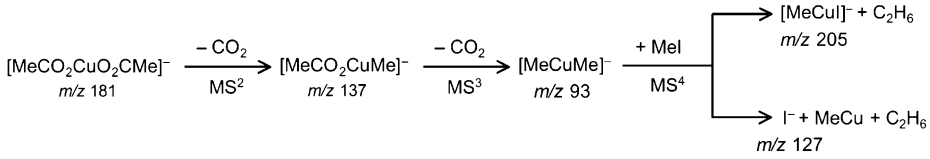

mental detail is necessary for both mechanistic and synthetic organocopper chemistry".[9]

An alternative approach to understanding the formation, stability, and reactivity of organocuprates is to study the gas-phase chemistry of well-defined organocuprate species, where the additional effects of solvent and counterions are absent and the possibility for dimerization and clustering is avoided. We have shown that the multistage mass spectrometry (MS^n) capabilities of the quadrupole ion trap (QIT) mass spectrometer provide opportunities to gain mechanistic insights into gas-phase metal-mediated chemistry.[10] Stable precursor ions can be transferred to the gas phase by electrospray ionization and then subjected to collision-induced dissociation (CID) to "synthesize" novel and reactive gas-phase ions. For example, decarboxylation of metal carboxylate anions can be used to synthesize organometallic species.[11,12] Indeed, the bare dimethyl cuprate anion $[MeCuMe]^-$ is readily formed via double decarboxylation of the copper acetate anion $[MeCO_2CuO_2CMe]^-$ using two stages of decarboxylation (Scheme 1).[11b] Importantly, similar dialkyl cuprate anions are too reactive to be generated directly by electrospray.[13] Moreover, despite the accepted experimental[14] and theoretical[15] paradigm that a dimer cluster $(R_2CuLi)_2$ is solely responsible for C−C bond coupling in the Corey−Posner reaction, we have demonstrated that gas-phase $[MeCuMe]^-$ undergoes C−C bond coupling with methyl iodide (Scheme 1).[11b]

Here we extend the scope of the double decarboxylation strategy to the formation of a variety of homo and hetero organocuprate anions shown in Scheme 2. The use of carboxylate ligands larger than acetate and containing different alkyl groups introduces a number of different reactions that might compete with decarboxylation; for example, loss of the carboxylate anion or elimination of alkenes via a β-hydride pathway.

Scheme 2

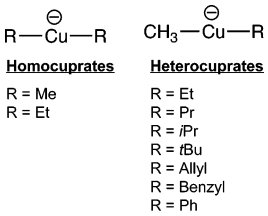

An additional complication for heterocarboxylate species is that decarboxylation might conceivably occur at either of the two different carboxylate ligands. These complications are illustrated in Scheme 3, which highlights possible competing fragmentation reactions of the simplest heterocarboxylate system $[MeCO_2CuO_2CEt]^-$.

There are four potential fragmentation pathways for the first stage of CID (MS^2): (i) decarboxylation at the acetate ligand to form $[MeCuO_2CEt]^-$, (ii) decarboxylation at the propionate ligand to form $[MeCO_2CuEt]^-$ (isomeric with $[MeCuO_2CEt]^-$), (iii) loss of the acetate anion $MeCO_2^-$ to form neutral CuO_2-CEt, and (iv) loss of the propionate anion $EtCO_2^-$ to form neutral CuO_2CMe. Similarly, the isomeric organocuprates $[MeCuO_2CEt]^-$ or $[MeCO_2CuEt]^-$ might then in turn fragment via different pathways in their MS^3 spectra. For example, while a second stage of decarboxylation would yield the same heterocuprate $[MeCuEt]^-$ for both isomers, $[MeCuO_2CEt]^-$ might be expected to undergo loss of propionate $EtCO_2^-$ while $[MeCO_2CuEt]^-$ might undergo loss of acetate $MeCO_2^-$. Furthermore, a new pathway is accessible for the $[MeCO_2CuEt]^-$ involving β-hydride transfer from the ethyl ligand and loss of

(6) The condensed phase decomposition reactions of alkyl organocopper compounds are complex and can involve β hydride transfer, radical reactions or reactions between ligands on adjacent metal centers: (a) Whitesides, G. M.; San Filippo, J.; Stedronsky, E. R.; Casey, C. P. *J. Am. Chem. Soc.* **1969**, *91*, 6542. (b) Whitesides, G. M.; Stedronsky, E. R.; Casey, C. P.; San Filippo, J. *J. Am. Chem. Soc.* **1970**, *92*, 1426. (c) Whitesides, G. M.; Panek, E. J.; Stedronsky, E. R. *J. Am. Chem. Soc.* **1972**, *94*, 232. (d) Wada, K.; Tamura, M.; Kochi, J. *J. Am. Chem. Soc.* **1970**, *92*, 6656. (e) Kochi, J. *Acc. Chem. Res.* **1974**, *7*, 351. (f) Miyashita, A.; Yamamoto, T.; Yamamoto, A. *Bull. Chem. Soc. Jpn.* **1977**, *50*, 1109. (g) Pasynkiewicz, S.; Poplawska, J. *J. Organomet. Chem.* **1985**, *282*, 427. (h) Pasynkiewicz, S.; Pikul, S.; Poplawska, J. *J. Organomet. Chem.* **1985**, *293*, 125. (i) Pasynkiewicz, S. *J. Organomet. Chem.* **1990**, *387*, 1. The nature of both the organic ligand and the auxiliary ligand can have a profound effect on the thermal stability of organocuprates: (j) van Koten, G.; James, S. L.; Jastrzebski, J. T. B. H. In *Comprehensive Organometallic Chemistry II: A Review of the Literature 1982−1994;* Abel, E. W., Stone, F. G. A., Wilkinson, G., Eds.; Pergamon: New York, 1995; Vol. 3, pp 75−77. (k) Bertz, S. H.; Dabbagh, G. *J. Chem. Soc., Chem. Commun.* **1982**, 1030.

(7) Thermal decomposition of certain unsaturated organocuprates gives the coupled product in high yield. (a) Whitesides, G. M.; Casey, C. P. *J. Am. Chem. Soc.* **1966**, *88*, 4541. (b) Kauffmann, T.; Sahm, W. *Angew. Chem., Int. Ed.* **1967**, *6*, 85. (c) Whitesides, G. M.; Casey, C. P.; Krieger, J. K. *J. Am. Chem. Soc.* **1971**, *93*, 1379.

(8) Oxidative decomposition reactions of organocuprates are being exploited in organic synthesis. For a review, see: Surry, D. S.; Spring, D. R. *Chem. Soc. Rev.* **2006**, *35*, 218.

(9) Bertz, S. H.; Human, J.; Ogle, C. A.; Seagle, P. *Org. Biomol. Chem.* **2005**, *3*, 392.

(10) O'Hair, R. A. J. *Chem. Commun.* **2006**, 1469.

(11) (a) O'Hair, R. A. J. *Chem. Commun.* **2002**, 20. (b) James, P. F.; O'Hair, R. A. J. *Org. Lett.* **2004**, *6*, 2761. (c) O'Hair, R. A. J.; Vrkic, A. K.; James, P. F. *J. Am. Chem. Soc.* **2004**, *126*, 12173. (d) Jacob, A.; James, P. F.; O'Hair, R. A. J. *Int. J. Mass Spectrom.* **2006**, *255−256*, 45. (e) O'Hair, R. A. J.; Waters, T.; Cao, B. *Angew. Chem., Int. Ed.* **2007**, *46*, 7048.

(12) Decarboxylation reactions have been used to synthesize organometallics in the condensed phase: (a) Deacon, G. B.; Faulks, S. J.; Pain, G. N. *Adv. Organomet. Chem.* **1986**, *25*, 237. Copper(I) salts can catalyze the decomposition of carboxylic acids: (b) Darensbourg, D. J.; Holtcamp, M. W.; Khandelwal, B.; Klausmeyer, K. K.; Reibenspies, J. H. *Inorg. Chem.* **1995**, *34*, 2389. Alkyne-stabilized monomeric copper(I) carboxylates undergo decarboxylation and can be used in a catalytic Hunsdiecker reaction: (c) Frosch, W.; Back, S.; Lang, H. *J. Organomet. Chem.* **2001**, *621*, 143.

(13) An alternative approach to generate organocuprate anions in the gas phase is direct electrospray of solutions of Gilman and related reagents, which yields the monomeric species $[CuR_2]^-$, $[RCuX]^-$, $[CuX_2]^-$ as well as higher clusters (X = Br, I, CN; R = thiophene, $(MeO)Me_2CCC$, Me_3SiCH_2): Lipshutz, B. H.; Keith, J.; Buzard, D. J. *Organometallics* **1999**, *18*, 1571. Attempts to generate mass spectra of the more basic alkyl homocuprates Me_2CuLi and nBu_2CuLi were not successful.

(14) (a) Pearson, R. G.; Gregory, C. D. *J. Am. Chem. Soc.* **1976**, *98*, 4098. The dimethyl cuprate anion $[MeCuMe]^-$ was reported to be unreactive toward simple electrophiles such as 1-dodecanylbromide in the condensed phase: (b) Mori, S.; Nakamura, E.; Morokuma, K. *J. Am. Chem. Soc.* **2000**, *122*, 7294.

(15) For theoretical studies relevant to C−C bond coupling with alkyl halides (the Corey−Posner reaction), see: (a) Mori, S.; Nakamura, E. *Tetrahedron Lett.* **1999**, *40*, 5319. (b) Mori, S.; Hirai, A.; Nakamura, M.; Nakamura, E. *Tetrahedron* **2000**, *56*, 2805. (c) Nakamura, E.; Mori, S.; Morokuma, K. *J. Am. Chem. Soc.* **1998**, *120*, 8273. (d) Nakamura, E.; Yamanaka, M.; Yoshikai, N.; Mori, S. *Angew. Chem., Int. Ed.* **2001**, *40*, 1935.

Scheme 3

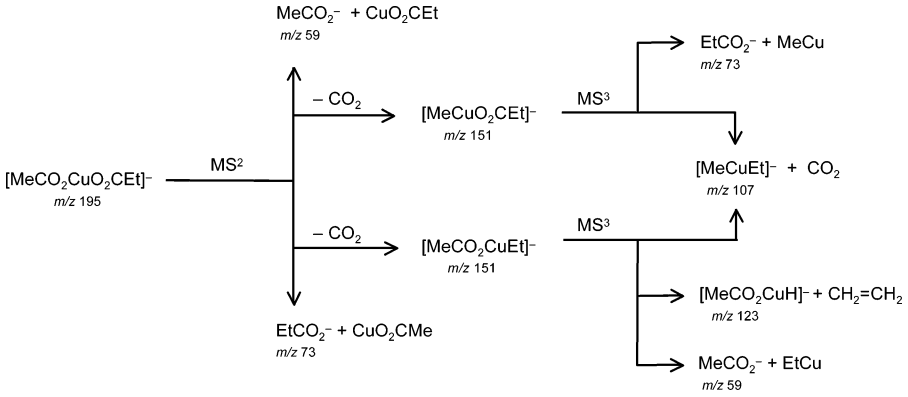

ethene to form $[MeCO_2CuH]^-$ (Scheme 3). To establish which of these classes of reactions operate, multistage mass spectrometry experiments were performed, including CID, isotope labeling, and ion−molecule reactions.[10] The experimental data were interpreted with the aid of theoretical calculations using density functional theory (DFT).

Experimental Section

Reagents. Copper(II) acetate, vinyl acetic acid, hydrocinnamic acid, propiolic acid, allyl iodide, iodomethane, and trimethyl acetic acid were obtained from Aldrich. Propionic acid, phenylacetic acid, and *n*-butyric acid were obtained from BDH Laboratory Supplies. Isobutyric acid and methanol were obtained from Ajax. Benzoic acid was obtained from May Baker. Propionic-2,2-d_2 acid and propionic-3,3,3-d_3 acid were obtained from Isotec. All chemicals were used without further purification.

Mass Spectrometry. Mass spectra were recorded using a Finnigan LCQ quadrupole ion trap mass spectrometer with a Finnigan electrospray ionization source. The instrument was modified to allow for ion−molecule reactions to be carried out.[16] Copper(II) acetate and various carboxylic acids were dissolved in methanol in a 1:2 molar ratio, with typical concentrations of 0.2−1.0 mM. These solutions were pumped via a syringe into the electrospray source at a rate of 5 μL/min. Typical electrospray source conditions involved needle potentials of 4.0−5.0 kV and a heated capillary temperature of 180 °C. The desired precursor ion was mass selected and subjected to CID using standard isolation and excitation procedures via the "advanced scan" function of the LCQ software. The copper isotope pattern (^{63}Cu, 69.2%, ^{65}Cu, 30.8%) was used to identify copper-containing species. Ion−molecule reactions were conducted with a typical concentration of neutral reagent in the trap of ca. 2×10^{10} molecules cm^{-3}. Gronert's pioneering studies demonstrated that ions undergoing ion−molecule reactions in the LCQ are essentially at room temperature.[17]

DFT Calculations. Theoretical calculations were carried out to provide insights into the mechanisms of the formation of the organocuprates studied. Calculations were carried out with the Gaussian 03 package using DFT at the B3LYP level.[18,19] The Stuttgart effective core potential (SDD) basis set was used for Cu and the 6-31+G* basis set for all remaining atoms (C, H, O).[20] Tests were conducted with different levels of theory and comparisons drawn with X-ray crystallographic data (Supporting Information Tables S1 and S2).[21,22] Comparisons of calculated and experimental Cu−O bond lengths of the simple copper carboxylate $[MeCO_2CuO_2CMe]^-$ are presented in Supporting Information Table S1,[21] while Cu−C bond lengths for the simple organocuprate $[MeCuMe]^-$ are presented in Supporting Information Table S2.[22] The B3LYP level of theory was found to yield values in reasonable agreement with experimental Cu−O and Cu−C bond lengths and was chosen on the basis of a compromise between accuracy and computational expense for calculations on the larger systems.

To evaluate the energies calculated at the B3LYP level of theory, we carried out single-point MP2 energy calculations on B3LYP-optimized structures (denoted MP2//B3LYP) on the double-decarboxylation reaction of the simplest carboxylate species $[MeCO_2CuO_2CMe]^-$. A comparison of relative energies at both levels is presented in Supporting Information Figure S1. The reasonable agreement between both levels of theory further supports the choice of the B3LYP level. Full data for each of the species mentioned in the text (including Cartesian coordinates, energies, and imaginary frequencies for transition states) are given in the Supporting Information (Figures S7−S20).

Results and Discussion

Electrospray of a copper(II) acetate $Cu(O_2CMe)_2$ solution in methanol resulted in a complex mass spectrum. Copper-containing species were identified by their characteristic isotope pattern (^{63}Cu, 69.2%, ^{65}Cu, 30.8%). An ion assigned to $[MeCO_2CuO_2CMe]^-$ (*m*/*z* 181) was observed in reasonable abundance and is presumably formed by reduction of $Cu(O_2CMe)_2$ during electrospray ($Cu^{II} \rightarrow Cu^{I}$). Multinuclear copper carboxylate cluster ions were also observed at higher *m*/*z*, but their gas-phase chemistry was not examined and thus they are not discussed here.

Different homo and hetero copper carboxylate species were generated by addition of different carboxylic acids to the electrospray solution. For example, addition of propionic acid resulted in a number of new copper-containing species being observed, including the homocarboxylate $[EtCO_2CuO_2CEt]^-$ (*m*/*z* 209) and the heterocarboxylate $[MeCO_2CuO_2CEt]^-$ (*m*/*z* 195).

The present approach to generating gas-phase organocuprates requires a double decarboxylation of copper carboxylate centers under low-energy CID conditions (Schemes 1 and 3). This method was adopted for the homocuprates derived from $[MeCO_2CuO_2CMe]^-$ and $[EtCO_2CuO_2CEt]^-$ and a series of

(16) Waters, T.; O'Hair, R. A. J.; Wedd, A. G. *J. Am. Chem. Soc*. **2003**, *125*, 3384.
(17) Gronert, S. *J. Am. Soc. Mass Spectrom.* **1998**, *9*, 845. (b) Gronert, S.; Pratt, L. M.; Mogali, S. *J. Am. Chem. Soc.* **2001**, *123*, 3081.
(18) Frisch, M. J.; et al. *Gaussian 03;* Gaussian, Inc.: Pittsburgh, PA, 2003.
(19) (a) Becke, A. D. *J. Chem. Phys.* **1993**, *98*, 5648. (b) Lee, C. T.; Yang, W. T.; Parr, R. G. *Phys. Rev. B* **1988**, *37*, 785.
(20) For a detailed discussion of basis sets for organocuprates, see: Yamanaka, M.; Inagaki, A.; Nakamura, E. *J. Comput. Chem.* **2003**, *24*, 1401.
(21) For an X-ray crystal structure of monomeric $[MeCO_2CuO_2CMe]^-$, see: Darensbourg, D. J.; Longridge, E. M.; Atnip, E. V.; Reibenspies, J. H. *Inorg. Chem.* **1992**, *31*, 3951.
(22) The structure of the simplest model system, the dimethyl cuprate ion $[MeCuMe]^-$, has been determined by X-ray crystallography. (a) Hope, H.; Olmstead, M. M.; Power, P. P.; Sandell, J.; Xu, X. *J. Am. Chem. Soc.* **1985**, *107*, 4337. (b) Dempsey, D. F.; Girolami, G. S. *Organometallics* **1988**, *7*, 1208.

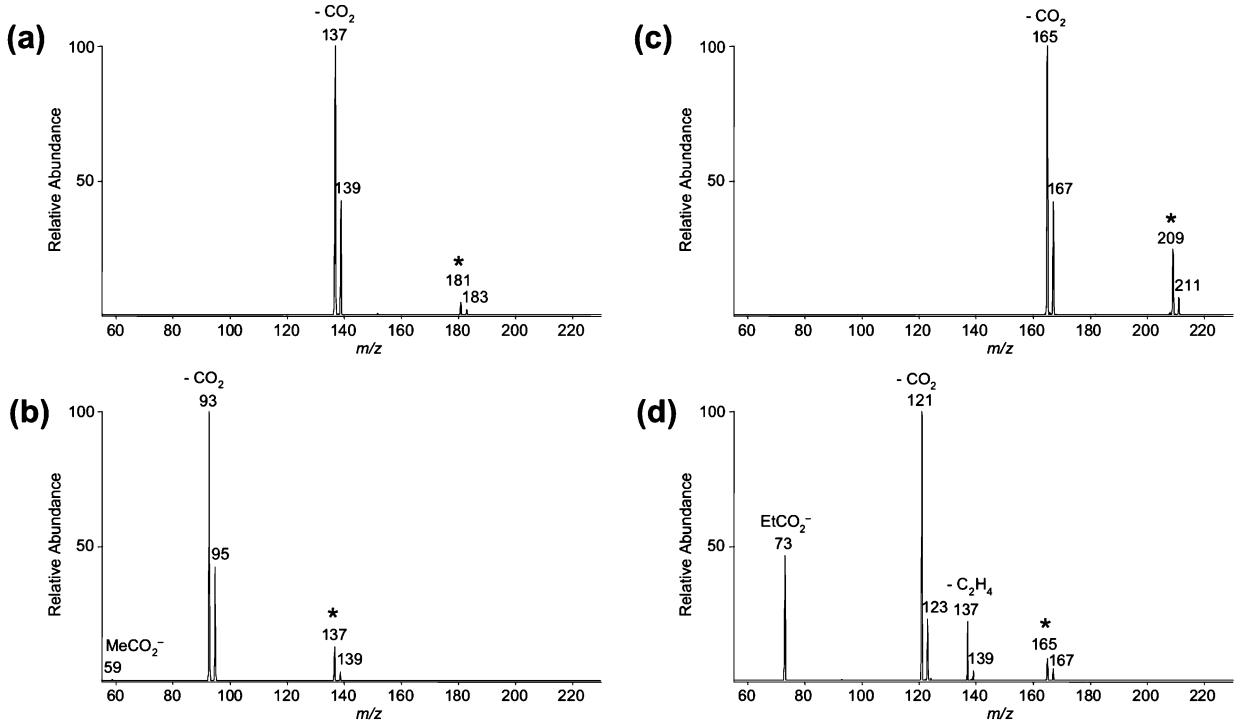

Figure 1. Mass spectra showing CID of the homocarboxylates $[MeCO_2CuO_2CMe]^-$ and $[EtCO_2CuO_2CEt]^-$. (a) MS^2 CID spectrum of $[MeCO_2CuO_2CMe]^-$, *m*/*z* 181. (b) MS^3 CID spectrum of $[MeCO_2CuMe]^-$, *m*/*z* 137. (c) MS^2 CID spectrum of $[EtCO_2CuO_2CEt]^-$, *m*/*z* 209. (d) MS^3 CID spectrum of $[EtCO_2CuEt]^-$, *m*/*z* 165. The mass-selected precursor ion is marked with an * in each case.

heterocuprates derived from $[MeCO_2CuO_2CR]^-$ (R = Et, Pr, *i*Pr, *t*Bu, allyl, benzyl, Ph; Scheme 2). Experimental and theoretical results are detailed in the following order: (i) formation of homo organocuprates $[MeCuMe]^-$ and $[EtCuEt]^-$ from $[MeCO_2CuO_2CMe]^-$ and $[EtCO_2CuO_2CEt]^-$, respectively, including a discussion of the competition between decarboxylation and other side reactions in their formation, and (ii) formation of hetero organocuprates $[MeCuR]^-$ from heterocarboxylate species $[MeCO_2CuO_2CR]^-$, including investigation of the site of the first decarboxylation ($MeCO_2^-$ or RCO_2^-) and the effect of R on the competition between decarboxylation and other possible side reactions.

(a) Formation of Homo Organocuprates $[MeCuMe]^-$ and $[EtCuEt]^-$. Decarboxylation of $[MeCO_2CuO_2CMe]^-$ and $[EtCO_2CuO_2CEt]^-$ to form $[MeCuMe]^-$ and $[EtCuEt]^-$, respectively, revealed that a number of different reactions were in competition with decarboxylation, including loss of the carboxylate anion and β-hydride transfer. The fragmentation reactions of $[MeCO_2CuO_2CMe]^-$ and $[EtCO_2CuO_2CEt]^-$ illustrate these different reaction pathways, and thus the experiments and calculations on these systems are described first.

$[MeCO_2CuO_2CMe]^-$. Collision-induced dissociation of $[MeCO_2CuO_2CMe]^-$ (*m*/*z* 181) resulted in formation of a peak at *m*/*z* 137 assigned to $[MeCO_2CuMe]^-$, arising from loss of neutral CO_2 (Figure 1a, eq 1). No other product ions were visible in the mass spectrum, indicating that loss of the acetate anion does not occur (eq 2). Theoretical results for this first decarboxylation reaction are given in Figure 2. The transition state for decarboxylation is 1.67 eV above the reactant species and is significantly favored over that for loss of an acetate ligand (2.68 eV, presumed to be barrierless). Since low-energy CID in the QIT tends to favor lower energy fragmentation reactions, the theoretically predicted preference for decarboxylation relative to loss of acetate is consistent with only decarboxylation being observed experimentally.

$$[MeCO_2CuO_2CMe]^- \rightarrow [MeCO_2CuMe]^- + CO_2 \quad (1)$$

$$\rightarrow MeCO_2^- + CuO_2CMe \quad (2)$$

CID of $[MeCO_2CuMe]^-$ (*m*/*z* 137) resulted in a second decarboxylation reaction, yielding the dimethyl cuprate anion $[MeCuMe]^-$ (*m*/*z* 93) (Figure 1b, eq 3). A very small amount of $MeCO_2^-$ (*m*/*z* 59) from acetate ligand loss was also observed (eq 4). The low mass cutoff of the ion trap meant that the possibility of methyl anion loss could not be detected (eq 5). Calculated relative energies for decarboxylation of $[MeCO_2CuMe]^-$ as well as loss of $MeCO_2^-$ are presented in Figure 2b. The relative energies predicted for these pathways are in agreement with the experimental results: the decarboxylation transition state is favored (1.67 eV, Figure 2b); however, loss of an acetate ligand is only slightly higher in energy (1.86 eV) and a small amount is observed experimentally. Loss of Me^- is predicted as much higher in energy (4.34 eV) and thus is not shown in Figure 2 and should not occur experimentally under conditions of low-energy collisional activation.

$$[MeCO_2CuMe]^- \rightarrow [MeCuMe]^- + CO_2 \quad (3)$$

$$\rightarrow MeCO_2^- + CuMe \quad (4)$$

$$\rightarrow Me^- + MeCO_2Cu \quad (5)$$

$[EtCO_2CuO_2CEt]^-$. Addition of propionic acid to the electrospray solution allowed $[EtCO_2CuO_2CEt]^-$ and $[MeCO_2CuO_2CEt]^-$ to be generated. The gas-phase chemistry

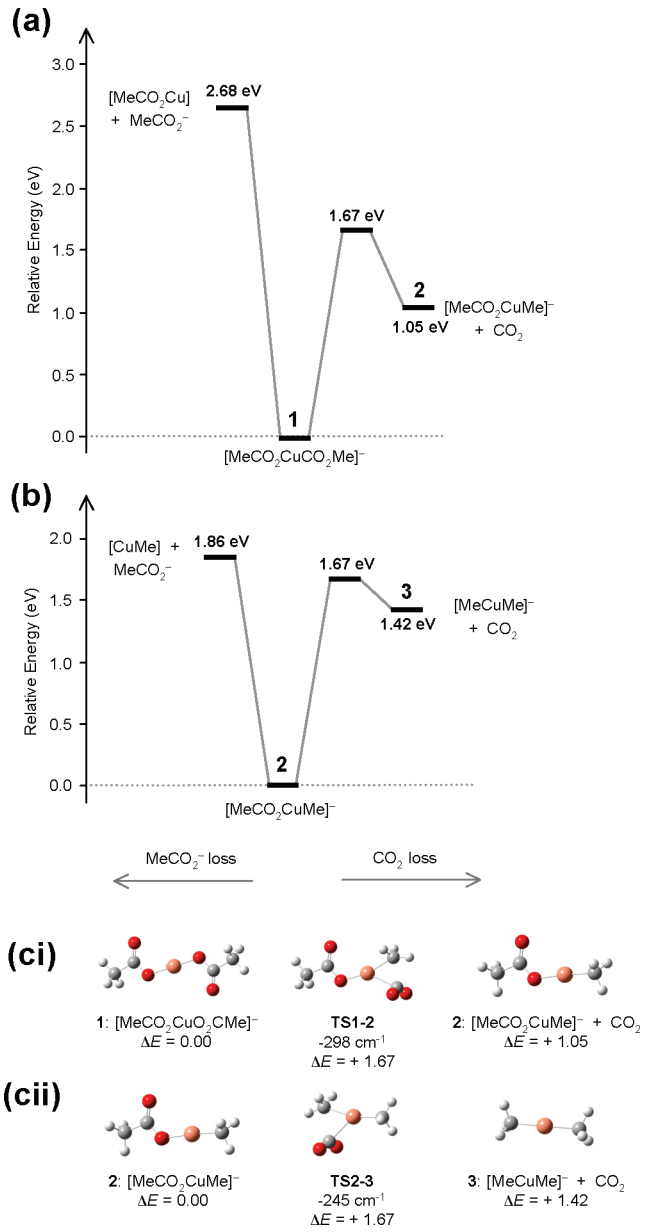

Figure 2. DFT-calculated energies for minima and transition states relevant to fragmentation of (a) $[MeCO_2CuO_2CMe]^-$ and (b) $[MeCO_2CuMe]^-$ via decarboxylation (right side) and acetate loss (left side). (c) Structures of minima and transition states relevant to the first (ci) and second (cii) decarboxylation pathway.

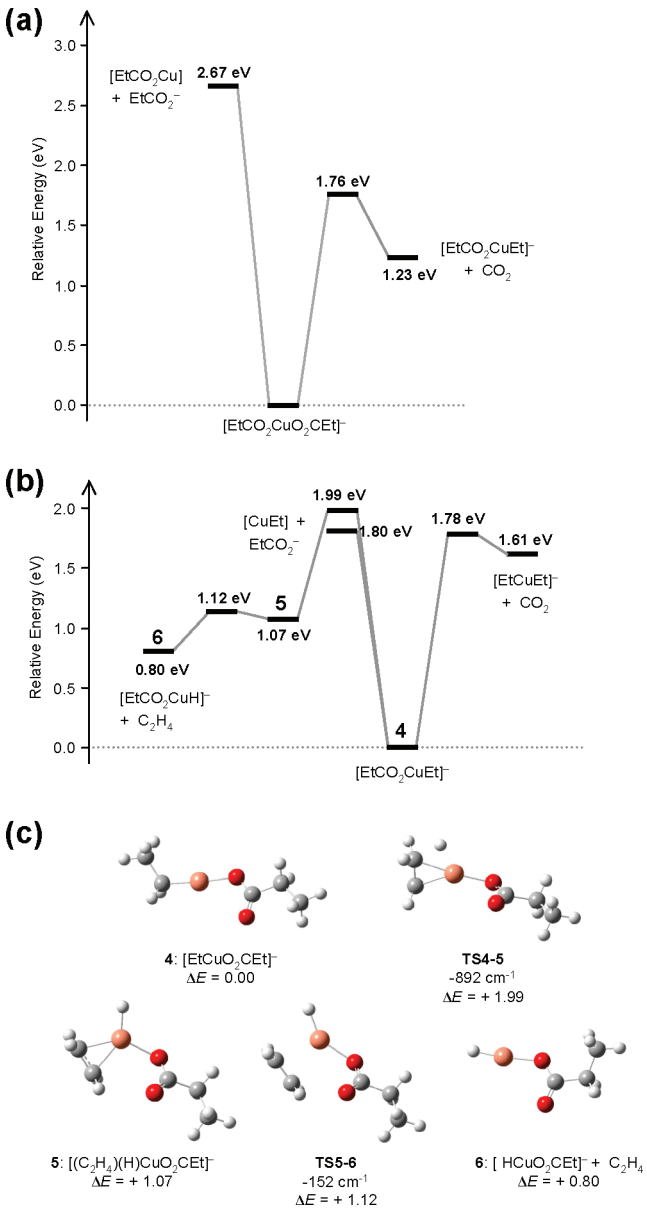

Figure 3. DFT-calculated energies for minima and transition states relevant to fragmentation of (a) $[EtCO_2CuO_2CEt]^-$ via decarboxylation (right side) and carboxylate loss (left side), (b) $[EtCO_2CuEt]^-$ via decarboxylation (right side) and carboxylate loss or β-hydride transfer (left side). (c) Structures of minima and transition states relevant to the β-hydride transfer pathway in (b).

of the latter ion is discussed in more detail below. CID of $[EtCO_2CuO_2CEt]^-$ (*m*/*z* 209) resulted in decarboxylation to yield $[EtCO_2CuEt]^-$ (*m*/*z* 165) (Figure 1c, eq 6). Again, no loss of $EtCO_2^-$ (*m*/*z* 73) was observed (eq 7). The DFT results summarized in Figure 3a reveal that the decarboxylation process is energetically favored over loss of the carboxylate, consistent with it being the dominant pathway observed experimentally.

$$[EtCO_2CuO_2CEt]^- \rightarrow [EtCO_2CuEt]^- + CO_2 \quad (6)$$

$$\rightarrow EtCO_2^- + CuO_2CEt \quad (7)$$

CID of the decarboxylation product $[EtCO_2CuEt]^-$ (*m*/*z* 165) resulted in three competing reactions (Figure 1d): (i) decarboxylation to yield $[EtCuEt]^-$ (*m*/*z* 121; eq 8), (ii) loss of $EtCO_2^-$ (*m*/*z* 73) to form neutral CuEt (eq 9), and (iii) loss of C_2H_4 to yield $[EtCO_2CuH]^-$ (*m*/*z* 137, eq 10). Once again, because of low mass cutoff of the ion trap, we were not able to detect ethyl anion loss (eq 11).

$$[EtCO_2CuEt]^- \rightarrow [EtCuEt]^- + CO_2 \quad (8)$$

$$\rightarrow EtCO_2^- + CuEt \quad (9)$$

$$\rightarrow [EtCO_2CuH]^- + C_2H_4 \quad (10)$$

$$\rightarrow Et^- + EtCO_2Cu \quad (11)$$

Formation of $[EtCO_2CuH]^-$ (*m*/*z* 137) is likely to occur by a β-hydride elimination reaction (eq 10). Two different deuterium labeling experiments were carried out to investigate this further: (i) CID of $[CH_3CD_2CO_2CuCD_2CH_3]^-$ yielded $[CH_3CD_2CO_2CuH]^-$, (*m*/*z* 139, eq 12; Supporting Information, Figure S2a), and (ii) CID of $[CD_3CH_2CO_2CuCH_2CD_3]^-$ yielded $[CD_3CH_2CO_2CuD]^-$ (*m*/*z* 141, eq 13; Supporting Information, Figure S2b). Both reactions support the β-position of the ethyl ligand as the origin of the hydride. This β-hydride elimination reaction is directly related to the thermal decomposition reaction of $Bu_3PCuCH_2CD_2CH_2CH_3$ studied by Whitesides et al. more than 30 years ago (eq 14).[6b]

$$[CH_3CD_2CO_2CuCD_2CH_3]^- \rightarrow [CH_3CD_2CO_2CuH]^- + CD_2{=}CH_2 \quad (12)$$

$$[CD_3CH_2CO_2CuCH_2CD_3]^- \rightarrow [CD_3CH_2CO_2CuD]^- + CH_2{=}CD_2 \quad (13)$$

$$Bu_3PCuCH_2CD_2CH_2CH_3 \rightarrow Bu_3PCuD + CH_2{=}CDCH_2CH_3 \quad (14)$$

DFT calculations relevant to fragmentation of $[EtCO_2CuEt]^-$ are summarized in Figure 3b,c. The calculated barriers for decarboxylation (1.78 eV, eq 8), loss of $EtCO_2^-$ (1.80 eV, eq 9), and β-hydride transfer (1.99 eV, eq 10) are all similar in energy, consistent with each pathway being observed experimentally. Loss of Et^- is again predicted to be much higher in energy and thus not expected to be observed experimentally (4.37 eV, eq 11). The initial product from β-hydride transfer has a side bound ethylene ligand (**5** of Figure 3c),[23] and thus a second lower energy transition state (**TS 5−6**) is required for loss of ethylene to form products $[EtCO_2CuH]^-$ and C_2H_4.

(b) Formation of Hetero Organocuprates $[MeCuR]^-$. The double decarboxylation of the heterocarboxylates $[MeCO_2CuO_2CR]^-$ was also investigated as a means of generating the heterocuprates $[MeCuR]^-$. For simplicity, we have maintained one ligand constant as acetate while varying the second carboxylate ligand (Scheme 2, R = Et, Pr, *i*Pr, *t*Bu, allyl, benzyl, Ph). This approach reduced the scope of species to be examined, while still allowing the effect of different alkyl and aryl ligands to be examined.

Overview of Competing Fragmentation Pathways. Results presented above for the homocarboxylates $[MeCO_2CuO_2CMe]^-$ and $[EtCO_2CuO_2CEt]^-$ suggested four possible competing fragmentation pathways might be expected for the heterocarboxylate systems $[MeCO_2CuO_2CR]^-$: decarboxylation from either of the two inequivalent carboxylate groups to yield isomeric species $[MeCuO_2CR]^-$ or $[MeCO_2CuR]^-$, respectively (eqs 15 and 16), or loss of either of the corresponding carboxylate anions $MeCO_2^-$ or RCO_2^- to yield neutral CuO_2CR or CuO_2CMe, respectively (eqs 17 and 18; e.g., Scheme 3 for $[MeCO_2CuO_2CEt]^-$).

$$[MeCO_2CuO_2CR]^- \rightarrow [MeCuO_2CR]^- + CO_2 \quad (15)$$

$$\rightarrow [MeCO_2CuR]^- + CO_2 \quad (16)$$

$$\rightarrow MeCO_2^- + CuO_2CR \quad (17)$$

$$\rightarrow MeCO_2Cu + RCO_2^- \quad (18)$$

Possible isomers arising from decarboxylation at the two different carboxylate ligands (i.e., $[MeCuO_2CR]^-$ and $[MeCO_2CuR]^-$) have the same molecular formula and thus cannot be distinguished directly via *m*/*z* values (eqs 15 and 16, respectively). The structure of these ions was instead examined by a combination of CID, ion−molecule reactions with allyl iodide, and DFT calculations. Results are presented in more detail for the simplest system $[MeCO_2CuO_2CEt]^-$, and then summarized below for larger systems $[MeCO_2CuO_2CR]^-$ (Scheme 2).

$[MeCO_2CuO_2CEt]^-$: Experiment and Theory. Possible pathways for the fragmentation of $[MeCO_2CuO_2CEt]^-$ are outlined in Scheme 3. CID of $[MeCO_2CuO_2CEt]^-$ (*m*/*z* 195) resulted in clean decarboxylation to yield a product ion at *m*/*z* 151, which might be assigned to either of the two isomers $[MeCuO_2CEt]^-$ or $[MeCO_2CuEt]^-$ (Figure 4a). Further fragmentation of the product ion at *m*/*z* 151 resulted in decarboxylation to yield $[MeCuEt]^-$ (*m*/*z* 107) along with some loss of $EtCO_2^-$ (*m*/*z* 73; Figure 4b). The loss of $EtCO_2^-$ is consistent with the presence of $[MeCuO_2CEt]^-$ rather than $[MeCO_2CuEt]^-$. Similarly, isomer $[MeCO_2CuEt]^-$ might be expected to undergo β-hydride elimination of C_2H_4, as observed for $[EtCO_2CuEt]^-$ (eq 10), and thus the fact that C_2H_4 loss is not observed might suggest that $[MeCO_2CuEt]^-$ is not present. However, the energy for decarboxylation might be lower than that for β-hydride elimination, and thus the absence of C_2H_4 loss does not rule out the presence of some $[MeCO_2CuEt]^-$ (see calculations below).

Reaction with allyl iodide was used as an alternative probe to test for the presence of the possible isomers $[MeCuO_2CEt]^-$ and $[MeCO_2CuEt]^-$ at *m*/*z* 151 (Figure 4c). The mass-selected product ion at *m*/*z* 151 reacted with allyl iodide by C−C coupling to generate the major product ion assigned to $[ICuO_2CEt]^-$ (*m*/*z* 263) with loss of neutral MeC_3H_5 (eq 19, R = Et). This indicated that the major portion of *m*/*z* 151 was $[MeCuO_2CEt]^-$ generated by initial decarboxylation of parent $[MeCO_2CuO_2CEt]^-$ at the acetate ligand. However, a much smaller signal was also observed for the formation of $[MeCO_2CuI]^-$ (*m*/*z* 249), arising from a C−C coupling reaction between $[MeCO_2CuEt]^-$ and allyl iodide with loss of neutral EtC_3H_5 (eq 20, R = Et). This indicated the presence of some of isomer $[MeCO_2CuEt]^-$ at *m*/*z* 151, generated by initial decarboxylation of parent $[MeCO_2CuO_2CEt]^-$ at the propionate ligand. The relative ratios of products $[ICuO_2CEt]^-$ and $[MeCO_2CuI]^-$ indicated that the majority of ion signal at *m*/*z* 151 corresponded to isomer $[MeCuO_2CEt]^-$, but with some of the alternative isomer $[MeCO_2CuEt]^-$ also present. Thus, the major site of decarboxylation of the parent $[MeCO_2CuO_2CEt]^-$ was the acetate ligand to generate $[MeCuO_2CEt]^-$, with only minor

(23) DFT calculations have identified a related isomer, $HCu(CH_2{=}CH_2)$, of ethyl copper(I): Bera, J. K.; Samuelson, A. G.; Chandrasekhar, J. *Organometallics* **1998**, *17*, 4136.

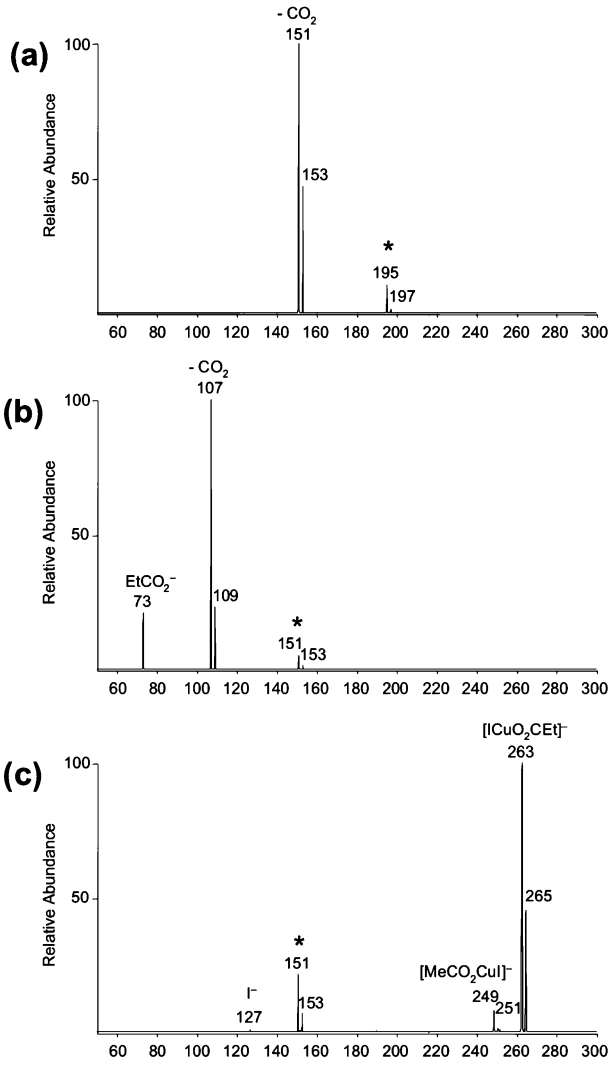

Figure 4. Fragmentation of the heterocarboxylate $[MeCO_2CuO_2CEt]^-$: (a) MS^2 spectrum showing CID of $[MeCO_2CuO_2CEt]^-$, (b) MS^3 spectrum showing CID of decarboxylated product from (a), (c) MS^3 spectrum showing ion−molecule reaction of decarboxylated product from (a) with allyl iodide (pressure = 2.5×10^{10} molecules cm^{-3}; reaction time = 5 s). The mass selected precursor ion is marked with an * in each case.

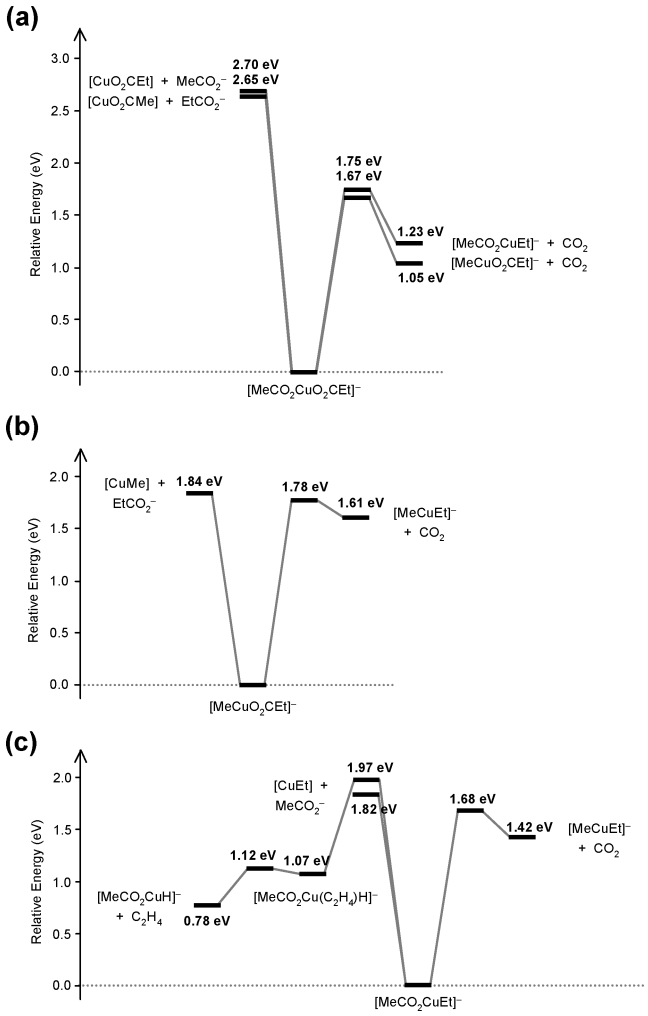

Figure 5. DFT-calculated energies for minima and transition states relevant to fragmentation of $[MeCO_2CuO_2CEt]^-$: (a) fragmentation of $[MeCO_2CuO_2CEt]^-$, (b) fragmentation of product $[MeCuO_2CEt]^-$ arising from decarboxylation of $[MeCO_2CuO_2CEt]^-$ at the acetate ligand, and (c) fragmentation of the alternative product $[MeCO_2CuEt]^-$ arising from decarboxylation of $[MeCO_2CuO_2CEt]^-$ at the propionate ligand.

decarboxylation occurring at the propionate ligand to generate $[MeCO_2CuEt]^-$.

$$[MeCuO_2CR]^- + C_3H_5I \rightarrow [ICuO_2CR]^- + MeC_3H_5 \quad (19)$$

$$[MeCO_2CuR]^- + C_3H_5I \rightarrow [MeCO_2CuI]^- + RC_3H_5 \quad (20)$$

The site of decarboxylation of $[MeCO_2CuO_2CEt]^-$ and the subsequent fragmentation reactions of the possible products $[MeCuO_2CEt]^-$ and $[MeCO_2CuEt]^-$ were also examined theoretically (Figure 5). DFT calculations indicated that the transition state for the initial decarboxylation at the acetate ligand was slightly favored over that for decarboxylation at the propionate ligand (1.67 and 1.75 eV above parent $[MeCO_2CuO_2CEt]^-$, respectively; Figure 5a). In addition, product $[MeCuO_2CEt]^-$ was also predicted to be favored over $[MeCO_2CuEt]^-$ on thermodynamic grounds (1.05 and 1.23 eV, respectively; Figure 5a). Loss of either $MeCO_2^-$ or $EtCO_2^-$ was much higher in energy (Figure 5a). The theoretical preference for product $[MeCuO_2CEt]^-$ is consistent with the experimental results; however, the similar energies of transition states are consistent with a smaller amount of the alternative product $[MeCO_2CuEt]^-$ also being observed (Figure 4c). The subsequent fragmentation reactions of the decarboxylated product (Figure 4b) are also consistent with the theoretically predicted fragmentation pathways of the isomers $[MeCuO_2CEt]^-$ and $[MeCO_2CuEt]^-$ (Figure 5b,c, respectively). In particular, decarboxylation is the lowest energy pathway for both isomers, consistent with it being the dominant pathway observed experimentally. Loss of $EtCO_2^-$ from $[MeCuO_2CEt]^-$ is predicted to be competitive with decarboxylation (1.84 vs 1.78 eV, respectively; Figure 5b), consistent with some $EtCO_2^-$ loss also being observed experimentally.

The ion−molecule reactions discussed above clearly demonstrate the presence of a minor component of isomer $[MeCO_2CuEt]^-$ along with the major isomer $[MeCuCO_2Et]^-$ (Figure 4c, eqs 19 and 20, R = Et). However, structurally diagnostic fragment ions for the minor component $[MeCO_2CuEt]^-$ were not observed (e.g., loss of $MeCO_2^-$ or loss of C_2H_4 to form $[MeCO_2CuH]^-$; Figure 4b). This indicated that decarboxylation to form $[MeCuEt]^-$ is preferred over these alternative pathways, and this was supported by the theoretical calculations

Table 1. DFT-Predicted Energies for Competing Decarboxylation (eqs 15 and 16) and Carboxylate Anion Loss (eqs 17 and 18) Reactions for $[MeCO_2CuO_2CR]^-$

R	$[MeCuO_2CR]^- + CO_2$[a] (eq 15)	$[MeCO_2CuR]^- + CO_2$[a] (eq 16)	$MeCO_2^- + CuO_2CR$[b] (eq 17)	$RCO_2^- + CuO_2CMe$[b] (eq 18)
Et	1.67 (1.05)	1.75 (1.24)	2.70	2.65
Pr	1.68 (1.05)	1.74 (1.18)	2.70	2.62
*i*Pr	1.67 (1.04)	1.86 (1.28)	2.70	2.60
*t*Bu	1.67 (1.03)	2.05 (1.24)	2.71	2.56
allyl	1.68 (1.03)	1.64 (0.86)	2.77	2.52
benzyl	1.68 (1.03)	1.59 (0.77)	2.78	2.39
Ph	1.68 (1.02)	1.53 (1.00)	2.78	2.42

[a] Activation energy (eV) for decarboxylation reactions (eqs 15 and 16). The values in parentheses refer to the overall endothermicity of the reaction. [b] Reaction endothermicity (eV) for carboxylate anion loss (assumed as barrierless, eqs 17 and 18).

(Figure 5c). Thus, both the β-hydride transfer reaction and $MeCO_2^-$ loss pathway are predicted to be higher in energy than decarboxylation, indicating that the small amount of $[MeCO_2CuEt]^-$ generated experimentally is likely to undergo decarboxylation rather than loss of $MeCO_2^-$ or β-hydride transfer.

Decarboxylation of $[MeCO_2CuO_2CR]^-$ (R = Pr, *i*Pr, *t*Bu, Allyl, Bz, Ph): Experiment and Theory. The site of the first decarboxylation reaction for the series $[MeCO_2CuO_2CR]^-$ (Scheme 2) was also examined experimentally and theoretically. DFT results for each of the four competing pathways (eqs 15−18) are described first to aid with an interpretation of the experimental results. The predicted activation energies for the two competing decarboxylation reactions (eqs 15 and 16) and endothermicities for two competing carboxylate anion losses (eqs 17 and 18) for each of $[MeCO_2CuO_2CR]^-$ are summarized in Table 1. Reaction endothermicities for the two competing decarboxylation reactions (eqs 15 and 16) are also included in parenthesis. Structures and energies for relevant species are given in the Supporting Information (S7−S20).

The theoretical results of Table 1 reveal several interesting trends: (i) the first decarboxylation step is predicted to be significantly favored over carboxylate anion loss for each of the systems (compare eqs 15 and 16 with eqs 17 and 18), (ii) although higher in energy than decarboxylation, loss of the RCO_2^- ligand is predicted to be favored over loss of the $MeCO_2^-$ ligand in each case (compare eqs 17 and 18), consistent with the enhanced acidities of RCO_2H over $MeCO_2H$,[24] (iii) the activation energy for decarboxylation at the acetate ligand of $[MeCO_2CuO_2CR]^-$ is virtually identical for all systems (eq 15; 1.67−1.68 eV), (iv) for each of the alkyl carboxylates (R = Et, Pr, *i*Pr, *t*Bu), the activation energy for decarboxylation from the RCO_2^- ligand is larger than that from the $MeCO_2^-$ ligand, and thus decarboxylation of these heterocarboxylates is predicted to yield mainly the $[MeCuO_2CR]^-$ isomer (eq 15), (v) the activation energy for decarboxylation from the RCO_2^- ligand of alkyl carboxylates increases in the order Me < Et < *i*Pr < *t*Bu (1.67, 1.75, 1.86, 2.05 eV, respectively), consistent with an increase in the steric bulk of the alkyl group, and (vi) systems with R = allyl, benzyl, and Ph have lower activation energies for decarboxylation at the RCO_2^- ligand than at the $MeCO_2^-$ ligand, and thus these are predicted to yield significant amounts of the $[MeCO_2CuR]^-$ isomer (eq 16).

The DFT calculations described above indicated that decarboxylation of $[MeCO_2CuO_2CR]^-$ at the $MeCO_2^-$ ligand was favored over that at the RCO_2^- ligand for each of R = Et, Pr, *i*Pr, and *t*Bu. In contrast, decarboxylation at the RCO_2^- ligand was predicted as favored for each of R = Ph, benzyl, and allyl. These predictions were tested experimentally using ion−molecule reactions with allyl iodide to probe for the presence of possible isomers $[MeCuO_2CR]^-$ and $[MeCO_2CuR]^-$, and thus establish the site of the first decarboxylation reaction. The results for two extreme cases $[MeCO_2CuO_2C\textit{t}Bu]^-$ and $[MeCO_2CuO_2CCH_2Ph]^-$ (Table 1) are shown in Figure 6. The experimental data support the theoretical results and confirm that the site of the first decarboxylation is dependent on the nature of the R group.

Calculations on the $[MeCO_2CuO_2C\textit{t}Bu]^-$ system with the bulky $\textit{t}BuCO_2^-$ ligand predicted that decarboxylation should occur at the acetate ligand rather than at the $\textit{t}BuCO_2^-$ ligand (transition states 1.67 and 2.05 eV above the reactant, respectively; Table 1). This was also supported by fragmentation and ion−molecule reactions of the product of initial decarboxylation (i.e., possible isomers $[MeCuO_2C\textit{t}Bu]^-$ or $[MeCO_2Cu\textit{t}Bu]^-$). CID of the decarboxylated product gave only $\textit{t}BuCO_2^-$, consistent with the presence of $[MeCuO_2C\textit{t}Bu]^-$ rather than the alternative isomer $[MeCO_2Cu\textit{t}Bu]^-$ (Figure 6b). Similarly, the ion−molecule reaction with allyl iodide resulted in exclusive formation of $[ICuO_2C\textit{t}Bu]^-$, again consistent with the presence of $[MeCuO_2C\textit{t}Bu]^-$ rather than $[MeCO_2Cu\textit{t}Bu]^-$ (Figure 6c, eq 19 where R = *t*Bu).

In contrast, calculations on the $[MeCO_2CuO_2CCH_2Ph]^-$ system predicted that decarboxylation should occur at the $PhCH_2CO_2^-$ ligand rather than at the $MeCO_2^-$ ligand (transition states 1.59 and 1.68 eV above the reactant, respectively). Collisional activation of $[MeCO_2CuO_2CCH_2Ph]^-$ resulted in decarboxylation in both the first and second stages of CID (Figure 6d,e, respectively). The absence of competing pathways in the second stage of decarboxylation meant that this reaction did not provide structural information about the product of initial decarboxylation. However, ion−molecule reactions with allyl iodide allowed the nature of this product to be examined. Accordingly, the ion assigned as either $[MeCO_2CuCH_2Ph]^-$ or $[MeCuO_2CCH_2Ph]^-$ reacted with allyl iodide to form mainly $[MeCO_2CuI]^-$ (via eq 20, R = CH_2Ph) and a much smaller amount of $[ICuO_2CCH_2Ph]^-$ (via eq 19, R = CH_2Ph). This indicated that decarboxylation of $[MeCO_2CuO_2CCH_2Ph]^-$ gave mainly $[MeCO_2CuCH_2Ph]^-$ from decarboxylation at $PhCH_2CO_2^-$ (Figure 6f). These results are consistent with the DFT predictions (Table 1).

The CID spectra of all remaining $[MeCO_2CuO_2CR]^-$ systems were also examined (Scheme 2, Supporting Information Figures S3−S6). The first stage of CID proceeded almost exclusively by the loss of CO_2, consistent with the DFT predictions (Table

(24) Caldwell, G.; Renneboog, R.; Kebarle, P. *Can. J. Chem.* **1989**, *67*, 611.

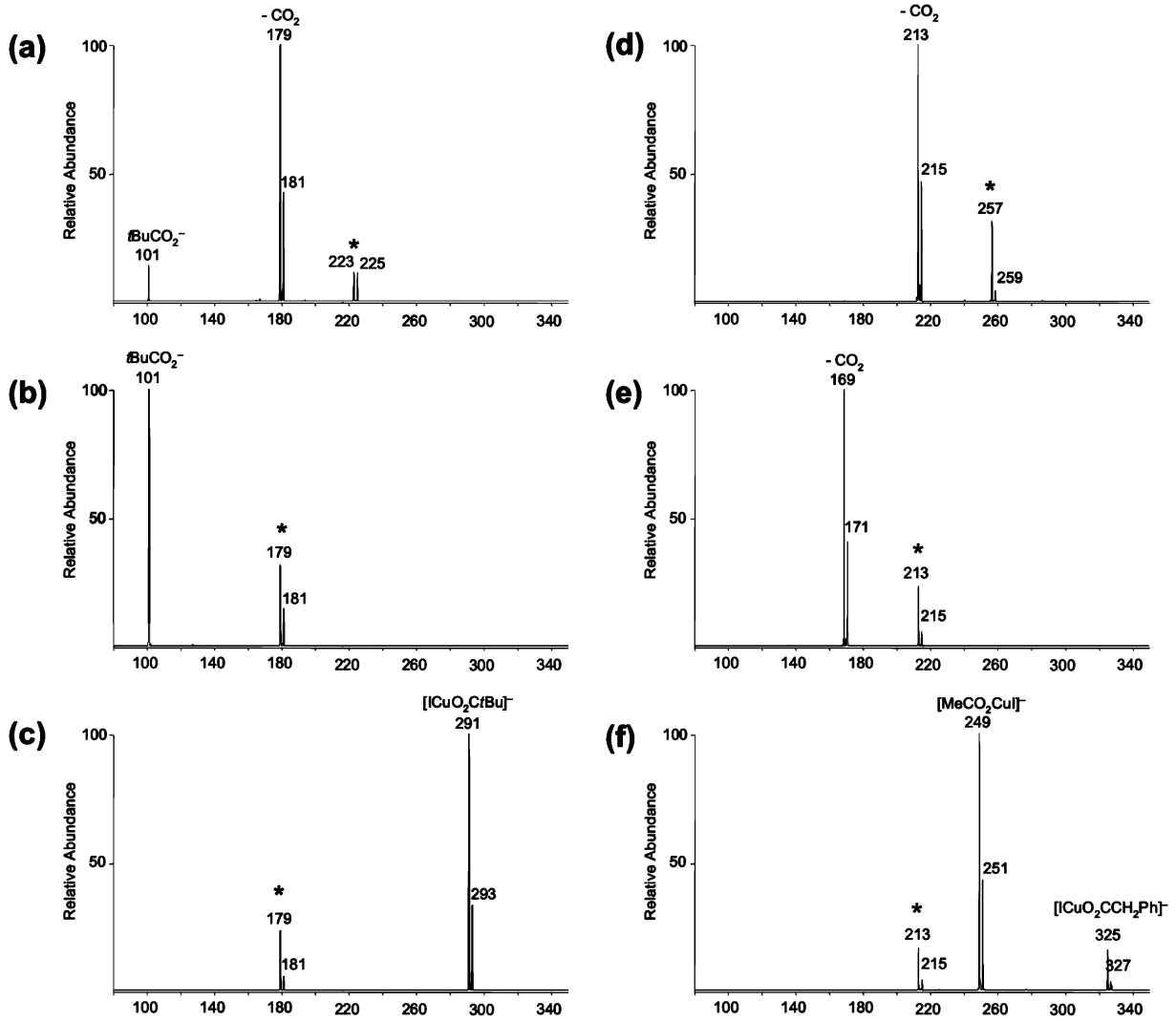

Figure 6. Fragmentation of the heterocarboxylates $[MeCO_2CuO_2CtBu]^-$ and $[MeCO_2CuO_2CCH_2Ph]^-$: (a) MS^2 spectrum showing CID of $[MeCO_2CuO_2CtBu]^-$ (*m*/*z* 223), (b) MS^3 spectrum showing CID of the decarboxylated product from (a) at *m*/*z* 179, (c) MS^3 spectrum showing ion−molecule reaction of decarboxylated product from (a) at *m*/*z* 179 with allyl iodide (pressure = 2×10^{10} molecules cm^{-3}; reaction time = 7 s), (d) MS^2 spectrum showing CID of $[MeCO_2CuO_2CCH_2Ph]^-$ at *m*/*z* 257, (e) MS^3 spectrum showing CID of decarboxylated product from (d) at *m*/*z* 213, (f) MS^3 spectrum showing ion−molecule reaction of decarboxylated product from (d) at *m*/*z* 213 with allyl iodide (pressure = 2×10^{10} molecules cm^{-3}; reaction time = 5 s). The mass-selected precursor ion is marked with an * in each case.

1, Figures S3a−S6a). Assignment of the initial site of decarboxylation via ion−molecule reactions with allyl iodide supported the DFT predictions. For example, in the case of R = Pr and *i*Pr, reaction of the product of initial decarboxylation (either $[MeCuO_2CR]^-$ or $[MeCO_2CuR]^-$) with allyl iodide revealed that the majority of initial decarboxylation occurred from the acetate ligand to form $[MeCuO_2CR]^-$, but that some decarboxylation also occurred at the RCO_2^- ligand to form $[MeCO_2CuR]^-$ (Figures S3c and S4c).

For the R = allyl system, reaction with allyl iodide indicated clean decarboxylation of parent $[MeCO_2CuO_2CC_3H_5]^-$ at the $C_3H_5CO_2^-$ ligand to yield $[MeCO_2CuC_3H_5]^-$ (eq 16, R = allyl). Similarly, for the R = Ph system, decarboxylation of $[MeCO_2CuO_2CPh]^-$ occurred predominantly from the $PhCO_2^-$ ligand (eq 16, R = Ph), but with some decarboxylation also occurring at the acetate ligand (eq 15). These experimental results are consistent with the DFT-predicted lowest energy decarboxylation pathways (Table 1), although there are some minor inconsistencies in the observed relative yields of the two isomers that might be expected on the basis of the relative energies of the DFT-predicted barrier heights.

As described above, decarboxylation at the RCO_2^- ligand of $[MeCO_2CuO_2CR]^-$ was preferred for each of R = Ph, benzyl, and allyl, indicating that the site of decarboxylation was dependent on additional factors aside from sterics. For example, this is most apparent by comparison of the theoretical results for $[MeCO_2CuO_2CPr]^-$ and $[MeCO_2CuO_2CCH_2Ph]^-$ (i.e., R = Pr and benzyl, respectively; Table 1). Decarboxylation at the $PrCO_2^-$ ligand of the former or the $PhCH_2CO_2^-$ ligand of the latter might be expected to involve similar activation barriers on the basis of sterics alone. However, the calculations predicted that the barrier for decarboxylation at $PrCO_2^-$ was higher than that for $PhCH_2CO_2^-$ (1.74 and 1.59 eV, respectively; Table 1). These results can be rationalized on the basis of differences in Cu−C bond strengths in the products of decarboxylation, that is, the stronger Cu−C bond of product $[MeCO_2CuCH_2Ph]^-$ relative to that of $[MeCO_2CuPr]^-$ results in a reduced activation barrier for the $PhCH_2CO_2^-$ ligand of $[MeCO_2CuO_2CCH_2Ph]^-$

Table 2. DFT-Predicted Energies for Competing Decarboxylation, Carboxylate Loss, and β-Hydride Transfer Reactions for Isomers $[RCO_2CuMe]^-$ and $[RCuO_2CMe]^-$

	products from $[MeCuO_2CR]^-$ isomer		products from $[MeCO_2CuR]^-$ isomer		
R	$[MeCuR]^- + CO_2$[a]	$RCO_2^- + CuMe$[b]	$[MeCuR]^- + CO_2$[a]	$MeCO_2^- + CuR$[b]	$[MeCO_2CuH]^- + R–H$[a]
Et	1.78	1.84	1.68	1.82	1.97
Pr	1.88	1.81	1.68	1.86	1.93
*i*Pr	1.91	1.80	1.68	1.83	1.98
*t*Bu	2.06	1.76	1.67	1.86	1.99
allyl	1.61	1.73	1.67	2.04	n/a
benzyl	1.56	1.61	1.67	2.12	n/a
Ph	1.58	1.64	1.71	2.25	n/a

[a] Activation energy (eV) for decarboxylation and β-hydride transfer reactions. [b] Reaction endothermicity (eV) for carboxylate anion loss (assumed as barrierless).

relative to that of the $PrCO_2^-$ ligand of $[MeCO_2CuO_2CPr]^-$ (Table 1). These different bond strengths are supported by the reduced endothermicity for formation of product $[MeCO_2CuCH_2Ph]^-$ from $[MeCO_2CuO_2CCH_2Ph]^-$ compared with product $[MeCO_2CuCH_2Et]^-$ from $[MeCO_2CuO_2CCH_2Et]^-$ (0.77 and 1.18 eV, respectively; Table 1). These data indicate that for the R = alkyl systems relative decarboxylation barriers are largely controlled by sterics, but that additional factors such as differences in Cu−C bond strengths are increasingly important for alternative systems such as R = allyl, benzyl, and phenyl.

Does the Double Decarboxylation Strategy Yield All Organocuprates, $[MeCuR]^-$? The theoretical and experimental results described above reveal that the activation energies for the competing channels of decarboxylation and carboxylate anion loss are dependent on the nature of R (Table 1). For example, for the $[MeCO_2CuO_2CtBu]^-$ system, initial decarboxylation is dominated by the formation of the $[MeCuO_2CtBu]^-$ isomer. However, this product does not undergo a second decarboxylation reaction, but rather fragments via loss of $tBuCO_2^-$ (Figure 6b). As a consequence, it was not possible to form the corresponding organocuprate $[MeCutBu]^-$ via the double decarboxylation strategy. Clearly, predicting whether it is possible to synthesize a given organocuprate $[MeCuR]^-$ from parent $[MeCO_2CuO_2CR]^-$ requires an understanding of which of the two possible isomers $[MeCuO_2CR]^-$ and $[MeCO_2CuR]^-$ is initially formed, as well as the fragmentation of this isomer, that is, whether it will undergo a second decarboxylation reaction.

The ability to form each of the organocuprates $MeCuR^-$ by the double decarboxylation strategy was assessed by a series of MS^3 CID experiments on the singly decarboxylated products generated from parent $[MeCO_2CuO_2CR]^-$. The experiments were supported by DFT calculations on both of the possible isomers $[MeCuO_2CR]^-$ and $[MeCO_2CuR]^-$. The experiments revealed that the products of CID of the singly decarboxylated product were dependent on the nature of the R group. For example, only decarboxylation occurred for R = benzyl, allyl, and Ph (Figure 6e, Supporting information Figures S5b and S6b, respectively). In contrast, no decarboxylation was observed for R = *t*Bu, and loss of $tBuCO_2^-$ was the sole channel observed (Figure 6b). The remaining R = alkyl cases (R = *i*Pr and Pr) were intermediate between these extremes and proceed by loss of both CO_2 and RCO_2^-, with the latter being the major product for R = *i*Pr. These results are consistent with the DFT calculations presented in Table 2: with increasing steric bulk of the alkyl group, the activation energy for decarboxylation increases, while the energy for RCO_2^- loss decreases because of increased stability of the carboxylate anion. As a consequence, carboxylate anion loss becomes increasingly competitive with decarboxylation for more bulky alkyl groups. Not surprisingly, the extreme case occurs for R = *t*Bu, and only carboxylate anion loss is observed from intermediate $[MeCuO_2CtBu]^-$. This means that $[MeCutBu]^-$ cannot be synthesized in the gas phase by the double decarboxylation strategy.

Conclusions

Decarboxylation of copper carboxylate anions represents a powerful method for the synthesis of organocuprate anions in the gas phase. Despite the possibility of a range of competing pathways, the activation energies for the double decarboxylation are sufficiently favorable to allow for the synthesis of eight of the nine organocuprates shown in Scheme 2. These include the two homocuprates $[MeCuMe]^-$ and $[EtCuEt]^-$, as well as a range of heterocuprates $[MeCuR]^-$ (R = Et, Pr, *i*Pr, allyl, benzyl, Ph). The only example for which the decarboxylation strategy was unsuccessful was $[MeCutBu]^-$. In this case, the increased steric bulk of the *t*Bu group disfavored the decarboxylation pathway and stabilized the carboxylate anion loss pathway such that intermediate $[MeCuO_2CtBu]^-$ underwent loss of $tBuCO_2^-$ rather than decarboxylation.

A key aspect of this work has been the combined use of experiments and theory to unravel the competing pathways in the formation of both the homo- and heterocuprates, in both the first and second decarboxylation steps. For example, decarboxylation of the heterocarboxylates $[MeCO_2CuO_2CR]^-$ can occur at either of the two different carboxylate ligands, giving rise to the possible isomers $[MeCuO_2CR]^-$ or $[MeCO_2CuR]^-$. The relative population of these isomers was established via ion−molecule reactions involving C−C coupling with allyl iodide, which produced either $[ICuO_2R]^-$ or $[MeCO_2CuI]^-$, respectively. This represents a rare example of how ion−molecule reactions can provide a means of distinguishing isomeric organometallic species in the gas phase.

An interesting pathway competing with the second decarboxylation was alkene loss by β-hydride transfer. For example, $[EtCO_2CuEt]^-$ underwent loss of C_2H_4 by β-hydride transfer to give $[EtCO_2CuH]^-$ as well as decarboxylation and $EtCO_2^-$ loss. This β-hydride transfer pathway parallels that established for $Bu_3PCuCH_2CD_2CH_2CH_3$ in solution (compare eqs 12 and 14). It is noteworthy that bond homolysis was not observed for any of the organocuprates $[MeCO_2CuR]^-$, suggesting that the complex decomposition reactions of organocuprates in solution may involve the intermediacy of cluster species.

Given the synthesis of the wide range of mononuclear organocuprates described in the present work, it will now be

possible to examine the inherent gas-phase reactivity of these homo- and heterocuprates in C−C bond coupling reactions with a range of electrophiles. It will be particularly interesting to compare how the selectivity of coupling (e.g., Me versus R groups) for the homocuprates $[MeCuR]^-$ changes as a function of the nature of the electrophile. Preliminary results suggest that the electrophile can have a profound influence on the outcome of C−C coupling. For example, $[MeCuPh]^-$ reacts with MeI to only give a product arising from C−C coupling between both methyl groups (eq 21, R = Me). The other cross-coupling (eq 22) and the homocoupling reaction (eq 23) were not observed. In contrast, each of the three possible C−C bond coupling products were observed in nearly equal abundance for allyl iodide, including both cross-coupling products (eqs 21 and 22, R = allyl) as well as the homocoupling reaction (eq 23, R = allyl). The formation of the homocoupling product is particularly interesting as it suggests the intermediacy of a Cu(III) π allyl intermediate.[25] Future work will address these differences in reactivity in more detail.

$$[MeCuPh]^- + RI \rightarrow [ICuPh]^- + MeR \quad (21)$$

$$\rightarrow [MeCuI]^- + PhR \quad (22)$$

$$\rightarrow [RCuI]^- + MePh \quad (23)$$

Acknowledgment. We thank the ARC for financial support of this work under the ARC Centres of Excellence program (ARC Centre of Excellence in Free Radical Chemistry and Biotechnology) and via Grants DP0558430 (to R.A.J.O.) and DP0772053 (to T.W.). VICS is acknowledged for the Chemical Sciences High Performance Computing Facility.

Supporting Information Available: Complete citation for ref 18. Comparison of experimental and theoretical Cu−O and Cu−C bond lengths for $[MeCO_2CuO_2CMe]^-$ and $[MeCuMe]^-$, respectively. Comparison of energies for decarboxylation of $[MeCO_2CuO_2CMe]^-$ at B3LYP//B3LYP and MP2//B3LYP levels of theory. Mass spectra for fragmentation of $[CD_3CH_2CuCH_2CD_3]^-$ and $[CH_3CD_2CuCD_2CH_3]^-$. Mass spectra for fragmentation and ion−molecule reactions of heterocarboxylate species $[MeCO_2CuO_2CR]^-$ mentioned in the text. Cartesian coordinates and energies (hartrees) for species relevant to each of the fragmentation pathways described in the text (Tables 1 and 2). This material is available free of charge via the Internet at http://pubs.acs.org.

JA0773397

(25) For previous studies that demonstrate the intermediacy of a Cu(III) π allyl intermediate in C−C bond coupling, see: (a) Karlström, A. S. E.; Bäckvall, J. E. *Chem.—Eur. J.* **2001**, *7*, 1981. (b) Norinder, J.; Bäckvall, J. E.; Yoshikai, N.; Nakamura, E. *Organometallics* **2006**, *25*, 2129.